

Photoluminescence and photocurrent characteristics of Eu^{2+} activated MAl_2O_4 ($\text{M} = \text{Ba}, \text{Ca}, \text{Sr}$) phosphors

Sei-Ki Kim · Mi-Jae Lee · Jong-Hoo Paik ·
Byung-Hyun Choi

Received: 28 June 2005 / Revised: 15 January 2006 / Accepted: 1 August 2006
© Springer Science + Business Media, LLC 2006

Abstract Photoluminescence and photocurrent characteristics of Eu^{2+} activated MAl_2O_4 ($\text{M} = \text{Ba}, \text{Ca}, \text{Sr}$) phosphors during and after Ultraviolet ray and visible light irradiation have been investigated. The photoluminescence (PL) and the photocurrent (PC) of the phosphors, in order to elucidate the relationship between the PL and the PC, were measured simultaneously on the same samples within a specially designed measuring box. Composition effects, such as a presence of Dy^{3+} as a co-activator and Al-rich composition on the PL and PC characteristics have been investigated. Also, sensing characteristics on UV and visual light have been tested.

The simultaneous measurement of PL and PC on the same sample clearly indicated that the presence of co-activator and vacant site, namely Al-rich composition, acted as a hole trap; the introduction of co-activator and vacant site decreased the PC and increased the PL during and after UV and visible light irradiation, whose PC was much lower than that of MAl_2O_4 with only Eu^{2+} as an activator. The electrical intensity affected on the PL characteristics after UV and visual light irradiation (afterglow); with increasing in the electrical intensity, the afterglow lasted more longer and intensively. The PC of MAl_2O_4 showed a good proportional relationship to UV and visible light intensity. Especially, SrAl_2O_4 showed an excellent linearity within $1\text{--}5 \text{ mW/cm}^2$, but showed somewhat delayed response and hysteresis as seen in CdS photoelectric cell.

Keywords MAl_2O_4 · Phosphor · Photoluminescence · Photocurrent · Sensor

1 Introduction

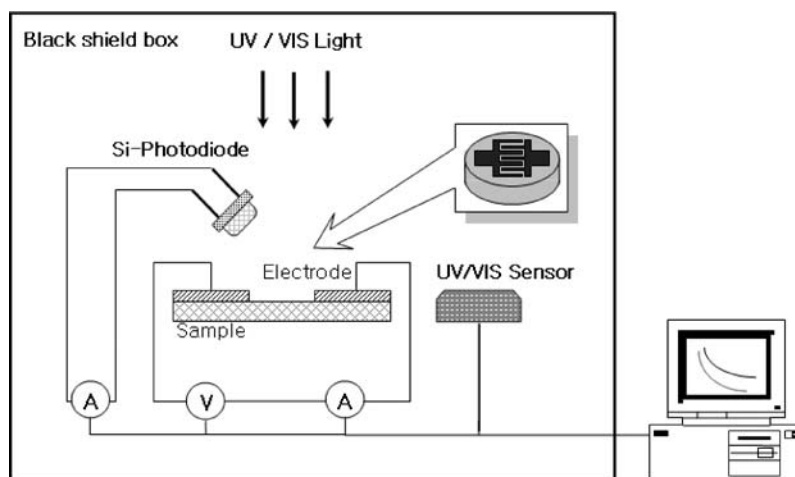
Eu^{2+} activated alkaline earth aluminates with the co-activators such as Dy for SrAl_2O_4 , Nd for BaAl_2O_4 and Nd, La for CaAl_2O_4 are well-known phosphors, which have a longer duration of photoluminescence and a higher brightness than traditional sulfide phosphors by 10–20 times [1–3]. The peak wavelength of emission spectra are 520 nm for $\text{SrAl}_2\text{O}_4:\text{Eu}$, 500 nm for $\text{BaAl}_2\text{O}_4:\text{Eu}$ and 440 nm for $\text{CaAl}_2\text{O}_4:\text{Eu}$ [4]. And the unusual long duration of photoluminescence of those aluminates offers a large field of applications [4–6]. As an explanation for the origin of the long duration of the photoluminescence, hole trapping and subsequent releasing of holes by thermal excitation was suggested [1]. In this case, the co-activators and crystallographic defects such as vacant sites act as a trapping center.

The aluminates phosphors are known to show similar behavior in the photoluminescence and photocurrent decay, and response to UV and visual light [3, 8, 9]. From the mechanism mentioned above, one can expect the photocurrent of those phosphors without the co-activator show a short decay time behavior. And it is expected that the photocurrent is strongly dependant on the host lattice, as is the case in the photoluminescence.

In this study, we have performed simultaneous measurement of photoluminescence (PL) and photocurrent (PC) on the same sample to elucidate the role of co-activator and vacant sites, and the effect of the host lattice of $\text{MAl}_2\text{O}_4:\text{Eu}$ ($\text{M} = \text{Sr}, \text{Ba}$ and Ca). And also, sensing characteristics to UV and visual light have been investigated.

S.-K. Kim (✉) · M.-J. Lee · J.-H. Paik · B.-H. Choi
Electronic Materials Technology Development Group,
Korea Institute of Ceramic Engineering and Technology, 233-5,
Gasam-Dong, Gueemcheon-Gu, Seoul 153-801, Korea
e-mail: kimseiki@kicet.re.kr

Fig. 1 Schematic diagram of measuring system of photoluminescence and photocurrent



2 Experimental

MAl_2O_4 : Eu(Dy, Nd, La) have been synthesized with 3N-grade MCO_3 ($\text{M} = \text{Sr, Ba, Ca}$), Eu_2O_3 , Dy_2O_3 , Nd_2O_3 , La_2O_3 and 4N-grade Al_2O_3 . The raw materials were mixed and thermally treated at 1200°C for 2 h in the air atmosphere with the agent of 8 mol.% B_2O_3 , and then ball-milled for 48h after crushing under $45\ \mu\text{m}$. The obtained powder were pressed into disk (Dia. 13 mm) and sintered at 1350°C for 2 h under a reducing atmosphere of 3% H_2 -Ar. XRD patterns of all of the synthesized compounds showed single phases in this study. Various electrode materials such as Ag, Au paste containing frit, sputtered Au and fritless Pt paste were tested on the sintered disks by sputtering and printing to the comb-like shape with the spacing of 0.3 mm.

Photoluminescence (PL) and photocurrent (PC) of the samples were measured simultaneously on the same samples within a specially designed measuring box as seen in Fig. 1; because MAl_2O_4 : Eu is sensitive to visual light, the measuring box was shielded from the external visual light. 20W-fluorescent lamps (Sankyo-denki, peak wavelength 368 nm, Japan) and D65 daylight fluorescent lamps (Gretagmacbeth, Canada) were used as a UV source and a visible light source, respectively. The UV and visual light intensity were controlled by adjusting the distance between light source and the sample according to the indication of UV radiometer (VLX-3W, Vilber Lourmat, France) and visible light meter (LX-1102, Lutron, Taiwan) placed beside the sample. The photocurrent was measured using high resistance meter (R8340A, ADVANTEST, Japan) with applied voltage of 0–30 V (R6144, ADVANTEST, Japan). The photoluminescence from the sample was measured using a digital multimeter (R6452, ADVANTEST, Japan) and Si-photodiode (S2386-45K, spectral response range 320–1100 nm, Hamamatsu Photonics, Japan), which was placed above the surface of the samples with a tilting angle of 45°C .

3 Results and discussions

The photocurrent according to the various electrode materials at the same condition showed the best results with fritless Pt paste; the resultant photocurrent was the most stable and the maximum value. So, the photocurrent measurements were conducted using fritless Pt paste hereafter.

Figure 2 shows the photoluminescence decay behavior of three types of composition; SrAl_2O_4 activated with only 1 at% Eu^{2+} , SrAl_2O_4 activated with 1 at% Eu^{2+} and 5 at% Dy^{3+} , and Al-rich composition of $(\text{Sr}_{0.99}\text{Eu}_{0.01})_{0.9}\text{Al}_2\text{O}_4$, which have vacant lattices in Sr sites. The sharp drop of PL after UV light off is seen in the composition without any co-activator and vacant sites; on the other hands, the compositions, which contain co-activator and/or vacant sites, show delayed decay behavior. The aspect of the delayed decay behavior in PL is more effective in Dy co-activated composition.

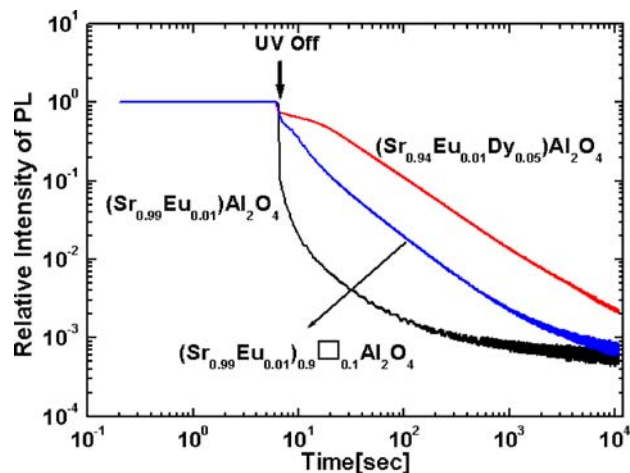


Fig. 2 Photoluminescence decay behavior of $(\text{Sr}_{0.99}\text{Eu}_{0.01})\text{Al}_2\text{O}_4$, $(\text{Sr}_{0.94}\text{Eu}_{0.01}\text{Dy}_{0.05})\text{Al}_2\text{O}_4$ and $(\text{Sr}_{0.99}\text{Eu}_{0.01})_{0.9}\text{Al}_2\text{O}_4$

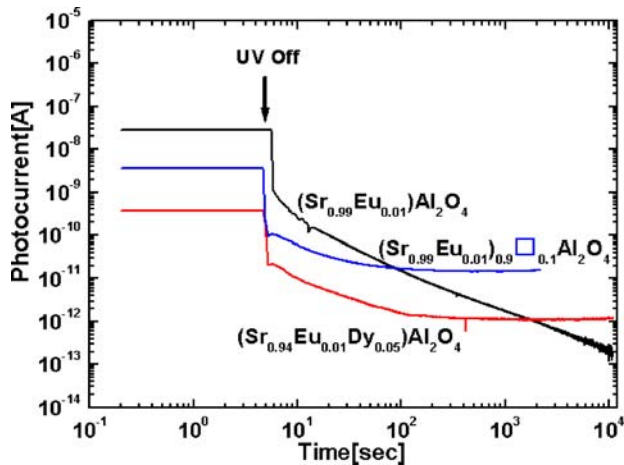


Fig. 3 Photocurrent decay behavior of $(\text{Sr}_{0.99}\text{Eu}_{0.01})\text{Al}_2\text{O}_4$, $(\text{Sr}_{0.94}\text{Eu}_{0.01}\text{Dy}_{0.05})\text{Al}_2\text{O}_4$ and $(\text{Sr}_{0.99}\text{Eu}_{0.01})_{0.9}\text{Al}_2\text{O}_4$

Figure 3 reveals the photocurrent decay behavior of three types of composition. It is found the photocurrent produced during UV light irradiation in $(\text{Sr}_{0.99}\text{Eu}_{0.01})\text{Al}_2\text{O}_4$ is higher than that of $(\text{Sr}_{0.99}\text{Eu}_{0.01})_{0.9}\text{Al}_2\text{O}_4$ by one order of magnitude, and higher than that of $(\text{Sr}_{0.94}\text{Eu}_{0.01}\text{Dy}_{0.05})\text{Al}_2\text{O}_4$ by two orders of magnitude. From the simultaneous measurement of photocurrent and photoluminescence on the same sample in this study, it is clear that co-activator and vacant sites act as trapping center, and capture the charge carriers of holes created in the valence band during excitation of Eu^{2+} .

Yuan et al. reported that the photocurrent of single-crystalline $(\text{Sr}_{0.99}\text{Eu}_{0.01})\text{Al}_2\text{O}_4$ was three orders of magnitude higher than that of single-crystalline $(\text{Sr}_{0.98}\text{Eu}_{0.01}\text{Dy}_{0.01})\text{Al}_2\text{O}_4$ [9]. Although the composition and measurement condition of photocurrent is different, it is thought that the smaller difference between the photocurrent of $(\text{Sr}_{0.99}\text{Eu}_{0.01})\text{Al}_2\text{O}_4$ and $(\text{Sr}_{0.94}\text{Eu}_{0.01}\text{Dy}_{0.05})\text{Al}_2\text{O}_4$ obtained in this study originates from defects; namely, there are more defects in polycrystalline sample than single crystal, and the defects

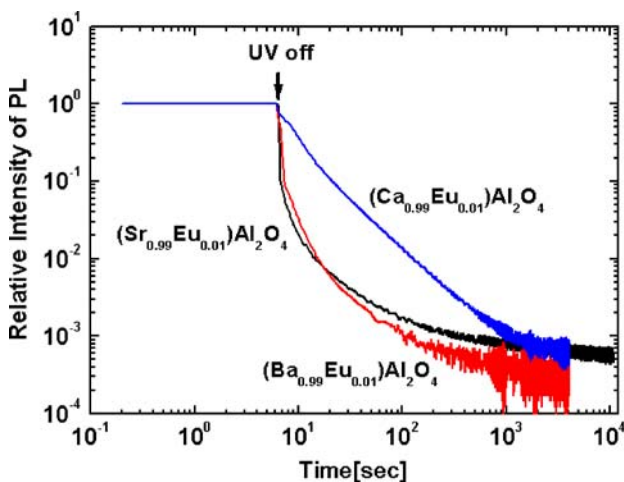


Fig. 4 Photoluminescence decay behavior of Eu^{2+} activated MAI_2O_4 ($M = \text{Sr}, \text{Ba}, \text{Ca}$)

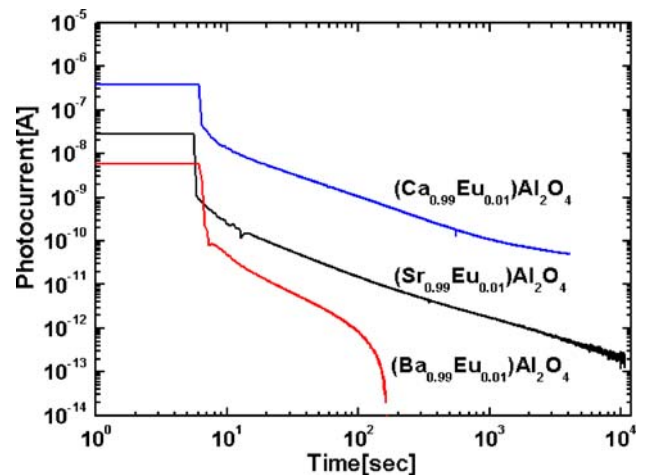


Fig. 5 Photocurrent decay behavior of Eu^{2+} activated MAI_2O_4 ($M = \text{Sr}, \text{Ba}, \text{Ca}$)

presents in both composition reduce the difference in the photocurrent.

Figure 4 shows the photoluminescence decay behavior of 1 at% of Eu^{2+} activated MAI_2O_4 ($M = \text{Sr}, \text{Ba}, \text{Ca}$). There are little difference in decay curves between $(\text{Sr}_{0.99}\text{Eu}_{0.01})\text{Al}_2\text{O}_4$ and $(\text{Ba}_{0.99}\text{Eu}_{0.01})\text{Al}_2\text{O}_4$, on the other hand, delayed decay behavior is observed in $(\text{Ca}_{0.99}\text{Eu}_{0.01})\text{Al}_2\text{O}_4$ composition without any co-activator. It is thought that the mechanism of long duration of photoluminescence may be much more complicated than simple adoption of trapping center.

Figure 5 shows the photocurrent decay behavior of 1 at% of Eu^{2+} activated MAI_2O_4 ($M = \text{Sr}, \text{Ba}, \text{Ca}$). The photocurrent generated during UV light irradiation in $(\text{Ca}_{0.99}\text{Eu}_{0.01})\text{Al}_2\text{O}_4$ is higher than that of $(\text{Sr}_{0.99}\text{Eu}_{0.01})\text{Al}_2\text{O}_4$ by one order of magnitude, and the current drop when UV light off is small.

After the current drop is occurred, the photocurrent of $(\text{Sr}_{0.99}\text{Eu}_{0.01})\text{Al}_2\text{O}_4$ and $(\text{Ca}_{0.99}\text{Eu}_{0.01})\text{Al}_2\text{O}_4$ decay linearly

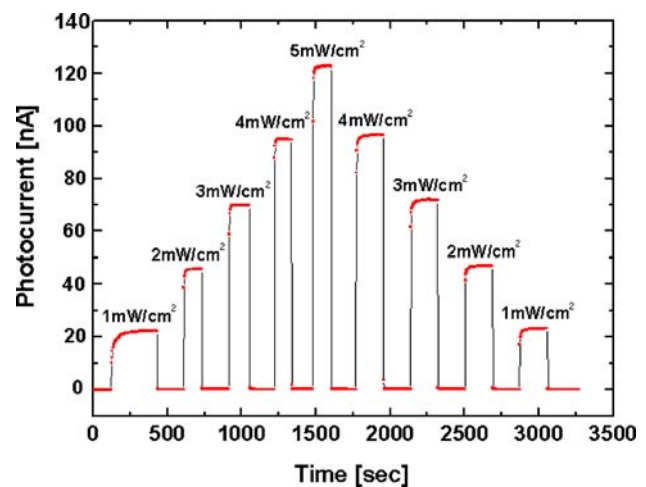
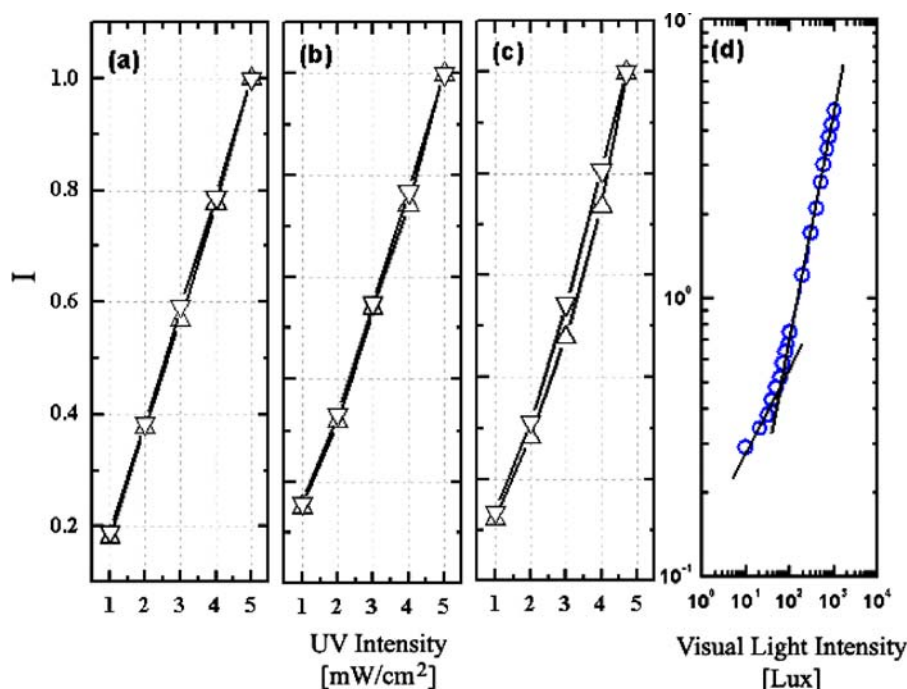


Fig. 6 UV light (peak wavelength 368 nm) response of $(\text{Sr}_{0.99}\text{Eu}_{0.01})\text{Al}_2\text{O}_4$

Fig. 7 Sensitivity of (a) $(\text{Sr}_{0.99}\text{Eu}_{0.01})\text{Al}_2\text{O}_4$, (b) $(\text{Ba}_{0.99}\text{Eu}_{0.01})\text{Al}_2\text{O}_4$ and (c) $(\text{Ca}_{0.99}\text{Eu}_{0.01})\text{Al}_2\text{O}_4$ composition to UV light, and (d) $(\text{Sr}_{0.99}\text{Eu}_{0.01})\text{Al}_2\text{O}_4$ to visible light of D65



with time. $(\text{Ba}_{0.99}\text{Eu}_{0.01})\text{Al}_2\text{O}_4$ composition shows very low photocurrent, and decays fast within about 2 min.

As shown in Fig. 6, $(\text{Sr}_{0.99}\text{Eu}_{0.01})\text{Al}_2\text{O}_4$ composition shows very good responsibility to UV light (peak wavelength of 368 nm); within the intensity of 1–5 mW/cm², the photocurrent shows fast responsibility and linearity (Fig. 7). And it is found that the weaker the UV intensity, the longer the response time.

Figure 7 shows the sensitivity of $(\text{Sr}_{0.99}\text{Eu}_{0.01})\text{Al}_2\text{O}_4$, $(\text{Ba}_{0.99}\text{Eu}_{0.01})\text{Al}_2\text{O}_4$ and $(\text{Ca}_{0.99}\text{Eu}_{0.01})\text{Al}_2\text{O}_4$ composition to UV light and visual light of D65 standard light source. The three compositions show linear responsibility to UV light, but $(\text{Ca}_{0.99}\text{Eu}_{0.01})\text{Al}_2\text{O}_4$ showed somewhat delayed response and hysteresis as seen in CdS photoconductive cell.

As shown in Fig. 7(d), $(\text{Sr}_{0.99}\text{Eu}_{0.01})\text{Al}_2\text{O}_4$ reveals the sensitivity to visual light; shows good linearity from 80 Lx to 1000 Lx, but the slope is changed in weaker intensity. The sensing characteristics of MAl_2O_4 (M = Sr, Ba, Ca) to visible light requires further studies.

4 Conclusions

The simultaneous measurement of photoluminescence and photocurrent on the same sample have been performed and clearly indicated that the presence of co-activator and vacant site, namely Al-rich composition, act as a hole trap. The hole

traps, which are introduced by the co-activator and/or vacant sites, capture the holes and result in the lower photocurrent. The captured holes in the hole traps are released thermally after light-off, and result in the higher photocurrent and photoluminescence.

$(\text{M}_{0.99}\text{Eu}_{0.01})\text{Al}_2\text{O}_4$ (M = Sr, Ba, Ca) shows very good responsibility to UV light (peak wavelength of 368 nm) within the intensity of 1–5 mW/cm² and the photocurrent shows fast responsibility and linearity, especially, $(\text{Sr}_{0.99}\text{Eu}_{0.01})\text{Al}_2\text{O}_4$ reveals the sensitivity to visible light; shows good linearity.

References

1. T. Matsuzawa, Y. Aoki, N. Takeuchi, and Y. Murayama, *J. Electrochem. Soc.*, **143**, 2670 (1996).
2. T. Katsumata, R. Sakai, S. Komuro, T. Morikawa, and H. Kimura, *J. Crystal Growth*, **198/199**, 869 (1999).
3. H. Yamamoto and T. Matsuzawa, *J. Luminescence*, **72–74**, 287 (1997).
4. F.C. Palilla, A.K. Levine, and M.R. Tomkus, *J. Electrochem. Soc.*, **115**, 643 (1968).
5. T. Katsumata, T. Nabae, K. Sasajima, S. Komuro, and T. Morikawa, *J. Electrochem. Soc.*, **144**, L234 (1997).
6. M. Kamada, J. Murakami and N. Ohno, *J. Luminescence*, **87–89**, 1042 (2000).
7. E. Nakazawa and T. Mochida, *J. Luminescence*, **72–74**, 236 (1997).
8. V. Abbruscato, *J. Electrochem*, **118**, 930 (1971).
9. H.B. Yuan, W. Jia, S.A. Basun, L. Lu, R.S. Meltzer, and W.M. Yen, *J. Electrochem. Soc.*, **147**, 3154 (2000).